Dielectric spectroscopy of a binary mixture of liquid crystals showing wide temperature range twisted grain boundary phase with re-entrant cholesteric phase

Meenal Gupta,[1] R. Dhar,[2,*] V. K. Agrawal,[1] R. Dabrowski,[3] and M. Tykarska[3]
[1]*Physics Department, University of Allahabad, Allahabad-211002, India*
[2]*Physics Department, Ewing Christian College, Allahabad-211003, India*
[3]*Institute of Chemistry, Military University of Technology, 00-908, Warsaw, Poland*
(Received 2 February 2005; published 9 August 2005)

There are only few materials, which have shown long temperature range twisted grain boundary (TGB) phases. One such material is the chiral binary mixture of 7OCB and 5* CBB (mole ratio 0.8 and 0.2) which shows unique phase sequence of cholesteric (N^*), a wide temperature range TGBA (~31 °C) and reentrant cholesteric (N^*_{re}) phases. In the present work we are reporting the dielectric spectroscopy of the above mixture with a chiral analog of earlier reported nematic (N), smectic-A (SmA), and reentrant nematic (N_{re}) phase sequences [Phys. Rev. A **46**, 7733 (1992)] for different conditions of molecular orientations. Two modes of dielectric relaxations have been detected in a homeotropically aligned sample with unusually low relaxation frequencies for one of them. Planar oriented molecules in the TGBA phase show a soft mode of relaxation and support the recently proposed theory for the soft mode relaxation of the TGBA phase [Phys. Rev. E **65**, 11701 (2001)]. By applying the dc electric field on planar oriented molecules in the TGBA phase, it has been possible to obtain a helix free homeotropically aligned TGBA phase.

DOI: 10.1103/PhysRevE.72.021703 PACS number(s): 61.30.Eb, 64.70.Md, 77.84.Nh

I. INTRODUCTION

The prediction of a twist grain boundary (TGB) phase by Renn and Lubensky in 1988 [1] and the subsequent realization by Goodby *et al.* in a pure system [2] and by Lavrentovich *et al.* in a mixture [3] have opened new vistas of research activities in the field of liquid crystals. Several types of TGB phases have been predicted, experimentally realized and their optical, thermodynamical, and structural properties have been extensively studied [4–18]. Detailed studies on different types of TGB phases are summarized in some recent review articles [19–22]. The simplest of these, the TGBA structure, consists of smectic slabs, separated by defect walls (grain boundaries) consisting of defect lines (twist dislocations) [14]. In the slabs, molecules are arranged in layers with their director normal to the smectic layers. Neighboring slabs (and hence the molecular director in the slabs) are twisted with respect to each other by angle $\Delta\chi$, thereby forming helical structure with the helix axis ($\vec{h}$) normal to the director [1,14]. A length along helical axis corresponding to the twist of smectic slabs (director) by angle 2π is the pitch of the TGB helix. The length of the smectic slabs (l_b), distance between defect lines (l_d), and pitch (P) are related by the equation

$$p = \Delta\chi/2\pi = l_b/P = 2\sin^{-1}(d/2l_d)/2\pi, \qquad (1)$$

where d is the layer spacing and p is a number. If p is irrational, the structure is incommensurate, i.e., there is no periodicity of the orientation of the slabs along the pitch axis, however, if p is rational, the system is commensurate and has n-fold screw axes. Several other TGB structures (TGBC, TGBC*, TGBQ, etc.) have also been proposed [4–6] and most of them have been experimentally realized [7–13]. In the proposed TGBC structure, the directors of the molecules in the smectic slabs are tilted with respect to the smectic layer normal [4,5]. In TGBC*, slabs are filled by SmC^* structure in such a way that helix of TGB structure is perpendicular to the helix of SmC^* structures [4,5]. Several other structures have been proposed for TGBC and TGBC* in a recent article by Brunet *et al.* [6].

The foremost requirements for the occurrence of TGB phases are the presence of strong chirality and weak layer structure. It is easier to incorporate these two properties in the binary systems by taking appropriate cholesteric and smectic compounds rather than in pure systems. Perhaps due to this reason, most often binary mixtures have shown TGB phases over a larger temperature range than those in pure systems [23–28].

Over the last 15 years since the recognition of TGB phases, several groups worldwide have written hundreds of papers on synthesis of the materials showing TGB phases and their optical, thermodynamical, and structural studies. However, there are very few studies reported on the static and dynamic dielectric properties of TGB phases [26,27,29–34]. Initial studies on frequency-dependent (dynamic) dielectric properties of the TGBA phase [29–33] show that, similar to those of the SmA^* phase, the electric field induces amplitude fluctuation of tilt angle and hence soft mode dielectric relaxation is observed in the TGBA phase. Similarly in the TGBC phase, electric field induces phase fluctuation of the tilt angle and hence a Goldstone mode of dielectric relaxation is observed similar to those in the SmC^* phase [33]. However, experimental evidence suggests that TGB phase relaxation processes have lower amplitudes and higher relaxation frequencies as compared to those observed in classical SmA^* and SmC^* phases. Ismaili *et al.*

*Email address: dr_ravindra_dhar@rediffmail.com

[35] have proposed a theoretical model verified by some experimental work as well, which suggests that Goldstone mode of TGBC and soft mode of TGBA phases are strongly reduced due to the existence of an elastic parameter (H_2) in these phases. Ismaili *et al.* have obtained the dielectric strength $(\delta\varepsilon_G)$ of Goldstone mode of TGBC and $(\delta\varepsilon_S)$ of soft mode of TGBA phase as [35]

$$\delta\varepsilon_G = \frac{\varepsilon_0 \chi_e^2 C^2}{\mathrm{H}_2} \cos\theta_S^2 \tag{2}$$

and

$$\delta\varepsilon_S = \frac{\varepsilon_0 \chi_e^2 C^2}{\alpha(T - T_C) + H_2} \tag{3}$$

with their respective relaxation frequencies as

$$f_G = \frac{H_2}{2\pi\gamma_G'} \tag{4}$$

and

$$f_S = \frac{\alpha(T - T_C) + H_2}{2\pi\gamma_S}, \tag{5}$$

where

$$H_2 = \frac{8\beta_a^2}{1 - \beta_a^2/3} \frac{K_{22}}{l_b^2}. \tag{6}$$

In Eqs. (2)–(6), θ_S is the spontaneous tilt angle of TGBC phase, C expresses the linear coupling between the tilt and the polarization, $T_C = T_0 + \varepsilon_0 \chi_e C^2/\alpha$ with T_0 representing Sm*A*-Sm*C* transition temperature in a nonchiral compound. Existence of H_2 is connected to the elastic distortion of the director and its amplitude depends strongly on the anchoring parameter (β_a) arising due to the anchoring forces at the grain boundaries and distance between the grain boundaries (l_b).

Experimental work carried out on dielectric properties of TGB phases so far, are on narrow temperature range TGBA and TGBC phases (~1–3 °C) mostly shown by ferroelectric liquid crystal (FLC) materials. We have carried out the frequency-dependent dielectric spectroscopy of a wide temperature range TGBA phase (~31 °C) observed in a binary mixture of 7OCB and 5^* CBB with a reentrant cholesteric phase [25] and the results are reported here. This mixture, however, does not possess a ferroelectric Sm-C^* phase and hence is different from previous dielectric spectroscopic studies of TGBA phase. It is also important to mention that phase sequence of this sample is a chiral analog of *N*-Sm-*A*-N_{re} for which dielectric spectroscopic results were reported earlier by Nozaki *et al.* [41].

II. MATERIAL

Present material has been taken from the system of binary mixtures of 7OCB and 5^* CBB studied and reported earlier by Brodzik and Dabrowski [25]. The phase diagram reported earlier [25] shows induction of a smectic A_d island surrounded by the TGBA phase in the concentration range of 20–60 mole % of 5^* CBB. For dielectric study, we have chosen a particular mixture having 20 mole % of 5^* CBB because this mixture shows a wide temperature range of TGBA phases (without any smectic phase) along with a reentrant cholesteric phase. The chemical structures of 7OCB and 5^* CBB are given below.

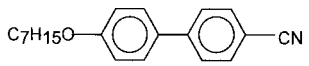

CHEMICAL STRUCTURE OF 7OCB

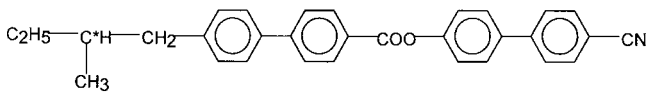

CHEMICAL STRUCTURE OF 5*CBB

This mixture shows the following phase sequence (with transition temperatures in °C) as observed under polarized light microscopy:

heating: $\mathrm{Cr} \underset{47°\mathrm{C}}{\rightarrow} \mathrm{TGBA} \underset{56°\mathrm{C}}{\rightarrow} N^* \underset{142.4°\mathrm{C}}{\rightarrow} I$

cooling: $I \underset{142.4°\mathrm{C}}{\rightarrow} N^* \underset{56°\mathrm{C}}{\rightarrow} \mathrm{TGBA} \underset{25°\mathrm{C}}{\rightarrow} N_{\mathrm{re}}{}^*$

The transitions $N_{\mathrm{re}}{}^* \leftrightarrow \mathrm{TGBA} \leftrightarrow N^*$ are of the second order. It is important to mention that different transition processes of this mixture are quite wide on the temperature scale as seen under polarizing microscope/DSC thermograms.

III. EXPERIMENTAL DETAILS

The complex dielectric permittivities $(\varepsilon^* = \varepsilon' - i\varepsilon'')$, in different mesophases of the homeotropic as well as planar aligned samples have been measured in the frequency range of 1 Hz to 10 MHz using a Solartron (SI-1260) impedance/gain phase analyzer, coupled with a Solartron dielectric interface (model-1296). The planar orientation of the sample has been achieved by depositing a thin layer of polyamide nylon onto ITO-coated glass electrodes (sheet resistance ~25Ω) and then rubbing the electrode surfaces unidirectionally with soft cotton. For a homeotropic alignment of the sample, electrodes were coated with the lecithin. Two plates of the dielectric cell were separated by Mylar spacers of thickness 10 μm in present studies. Dielectric cells (active capacitance ~100 pF) were calibrated at room temperature by using standard liquid cyclohexane. The temperature of the sample for optical and dielectric studies has been controlled by using a hot stage (Instec, model HS-1) having accuracy of ±0.1 °C and resolution limit 0.003 °C. The temperature near the sample was determined by the measuring the thermo-emf of a copper-constantan thermocouple using a six and half digit multimeter. Dielectric data have been acquired during cooling of the sample from its isotropic phase. Instrumental uncertainty in the basic measurement of capacitance (C) and conductance (G) in the frequency range concerned is less than 0.2% and hence uncertainty in the determination of permittivity (ε') and loss (ε'') from C and G is less than ±1%.

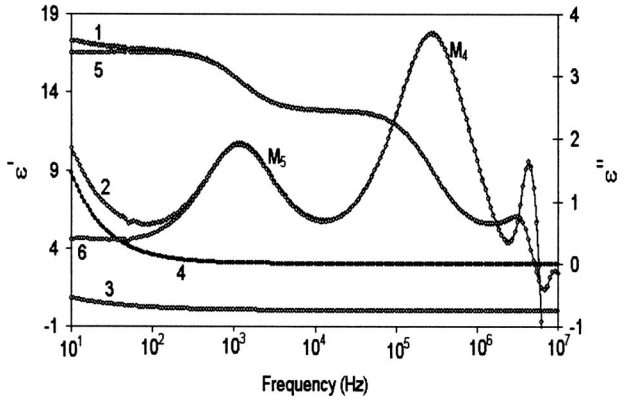

FIG. 1. Demonstration of low-frequency corrections from the measured relative dielectric permittivity ε' (curve 1) and loss ε'' (curve 2) data acquired for TGBA phase (31.7 °C) with a dc electric field of strength 30 kV/cm applied across planar cell. Curves 3 and 4 represent A_1/ω'' and $\sigma(\mathrm{dc})/\varepsilon_0\omega$ terms, respectively, obtained by fitting Eq. (7) with the measured data. Curves 5 and 6 represent corrected values of ε' and ε'' [after the subtraction of A_1/ω'' and $\sigma(\mathrm{dc})/\varepsilon_0\omega$ terms from the measured data] which seems free from artifacts in the frequency range of 10 Hz to 1 MHz. However, in the case of dielectric cells having homeotropic alignment of the sample, correction terms are very large and hence lower limit is reliable only up to 100 Hz.

Other details of the experimental techniques have been discussed elsewhere [36,37].

In the case of the present sample, measured dielectric data below 1 kHz are affected due to ionic conductance and electrode polarization effect [37] whereas data above 100 kHz are affected due to the combined effect of lead inductances and electrode surface resistances [38,39]. In order to remove low- and high-frequency artifacts from the measured data, the dielectric spectra have been fitted with the generalized Cole-Cole equation [40] using ORIGIN software,

$$\varepsilon^* = \varepsilon' - j\varepsilon'' = \varepsilon'(\infty) + \sum_i \frac{(\delta\varepsilon)_i}{1 + (j\omega\tau_i)^{(l-h_i)}} + \frac{A_l}{\omega^n} + \frac{\sigma(\mathrm{dc})}{j\varepsilon_0\omega} - jA\omega^m, \tag{7}$$

where $\varepsilon'(\infty)$ is the relative permittivity in the high-frequency limit and $\delta\varepsilon_i, \tau_i$, and h_i are the dielectric strength, the relaxation time (inverse of angular relaxation frequency), and symmetric distribution parameter ($0 \leqslant h_i \leqslant 1$) of ith mode, respectively. A_l, n, A, and m are constants. $\sigma(\mathrm{dc})$ is the ionic conductance and ε_0(=8.85 pF/m) is the free space permittivity. After subtracting low- and high-frequency correction terms from the measured data, it has been possible to explore different relaxation phenomenon in the frequency range of 10 Hz to 1 MHz as shown in Fig. 1 and hence characteristic parameters of different relaxation modes in different mesophases have been determined. Maximum uncertainties in the determination of relaxation frequencies and dielectric strengths of different relaxation modes by the process of fitting operations are about ±3.5 and ±1.5 %, respectively.

IV. RESULTS AND DISCUSSION

Present experimental work has been carried out in three different conditions and accordingly results have been reported and discussed in three subsections. In the first two sections (A and B), we have reported results on homeotropic and planar aligned samples obtained by the surface treatment of the electrodes. In the third section (C), effects of the dc electric field on the dielectric cells prepared for homeotropic and planar alignments of the samples (used in Secs. A and B) have been reported. In the last paragraph of this section, variations of static dielectric permittivies as determined in the homeotropic and planar configuration of molecules have been reported and discussed.

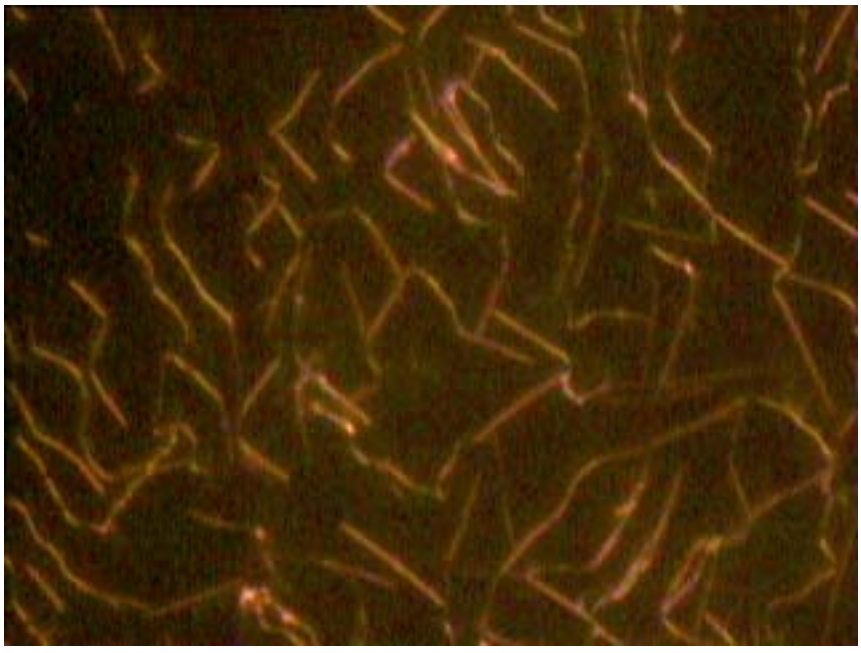

FIG. 2. (Color online) Filamentary texture of TGBA phase (36.2 °C) obtained for the homeotropic alignment of the sample.

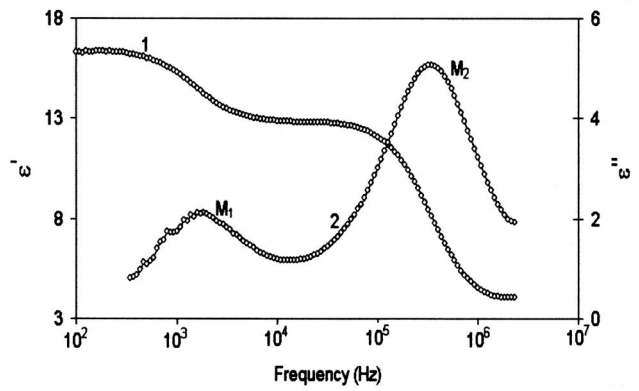

FIG. 3. Variation of relative dielectric permittivity $\varepsilon'_{\parallel}$ (curve 1) and loss $\varepsilon''_{\parallel}$ (curve 2) for homeotropic aligned sample in TGBA phase (31.7 °C) showing modes M_1 and M_2. Due to heavy dominance of ionic conductance in the low frequency region and weak strength of $M_1, \varepsilon''_{\parallel}$ data could not be corrected below 300 Hz.

A. Homeotropic aligned sample

In the case of homeotropic alignment, helical axes of N^* and TGBA phases lie parallel to the electrode surfaces. With proper homeotropic alignment, the TGBA phase shows filamentary texture as shown in Fig. 2. Corrected permittivity and loss data do not show any relaxation phenomena in the isotropic liquid phase. However, when the sample is cooled to a cholesteric phase, a weak relaxation mode named $M_1(\delta\varepsilon_1 \sim 1.7)$ appears at about 99 °C with its relaxation frequency at 282 kHz. Another mode of relaxation named $M_2(\delta\varepsilon_2 \sim 9.0)$ appears at about 54 °C, i.e., just below the N^*-TGBA transition with its relaxation frequency at 1.89 MHz. Simultaneous existences of both the modes are shown in Fig. 3 and 4 for TGBA phase at 31.7 °C. Temperature dependences of the relaxation frequencies (f_{r1} and f_{r2}) of these two modes are shown in Fig. 5, whereas Fig. 6 shows variations of their dielectric strengths ($\delta\varepsilon_1$ and $\delta\varepsilon_2$). As shown in Figs. 5 and 6, both modes continue to exist up to the lowest temperature of the measurement in the reentrant cholesteric phase and their relaxation frequencies follow a Arrhenius behavior [40]:

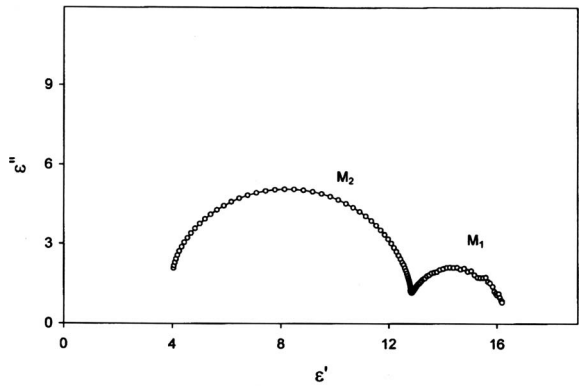

FIG. 4. Cole-Cole plot showing modes M_1 and M_2 of the homeotropic aligned sample in TGBA phase at 31.7 °C.

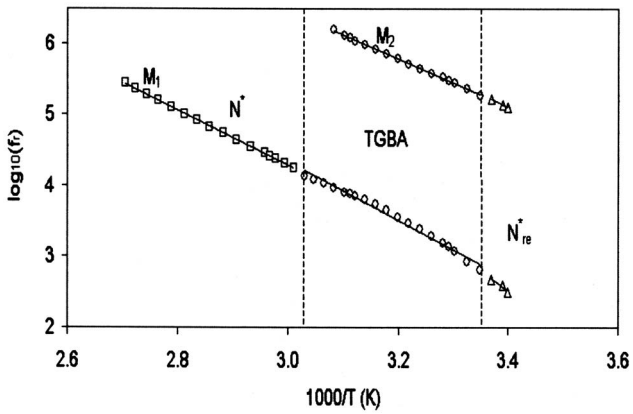

FIG. 5. Variation of relaxation frequencies of modes M_1 and M_2 with inverse of the temperature for the homeotropic aligned sample. Broken vertical lines represent different transition temperatures as reported in Sec. II.

$$f_r = A \exp(-W_a/kT), \tag{8}$$

where k is Boltzman constant and W_a is the activation energy. For both the modes (M_1 and M_2), variations of $\ln(f_r)$ with $1/T$ follow straight lines with different slopes in different phases (see Fig. 5). By using the method of least square fit, slopes of the straight lines from $\ln(f_r)$ versus $1/T$ plot and hence activation energies of dipolar rotation in N^*, TGBA, and $N_{re}{}^*$ phases have been determined. Activation energies thus determined are listed in Table I. The nature of the molecular alignment (homeotroic), fitting of the dielectric data on Cole-Cole arc, temperature dependence of relaxation frequencies, and magnitude of activation energies in different mesophases suggest that both these modes arise due to the rotation of individual molecules about their short axes [41–43]. However, there are certain issues need to be addressed.

(1) Why are there two modes of relaxations corresponding to the rotation of molecules about their short axes against the usual single mode?

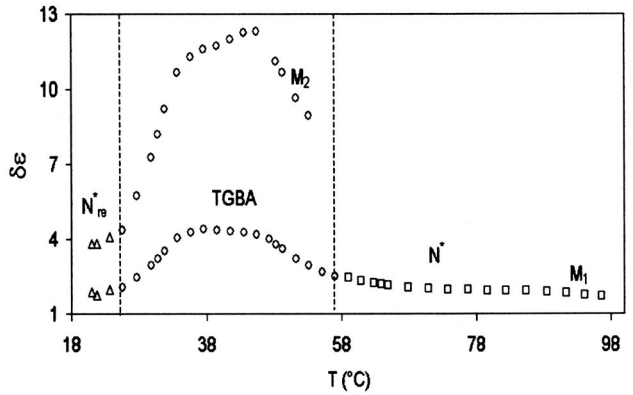

FIG. 6. Variation of dielectric strengths of modes M_1 and M_2 with temperature for the homeotropic aligned sample. Broken vertical lines represent different transition temperatures as reported in Sec. II.

TABLE I. Activation energy (W_a) in eV for different mesophases obtained from the Arrhenious plot.

Phases (mode)	Homeotropic cell	Planar cell with dc field
N^* (M_1)	0.77	0.70
TGBA (M_1)	0.81	0.85
TGBA (M_2)	0.68	0.71
N^*_{re} (M_1)	1.1	[a]
N^*_{re} (M_2)	0.8	[a]

[a]Number of measurements not sufficient to find W_a.

(2) Why has M_1 not been observed in the higher temperature side of a N^* phase lying above 98 °C? Further, M_2 has not been observed in the entire temperature range of N^* phase.

(3) Relaxation frequencies of M_2 varies from 1.89 MHz at 54 °C to 125 kHz at 21 °C, which is usual range for relaxation frequencies corresponding to rotation of molecules about their short axes. However, the relaxation frequency range of M_1 starting from 282 kHz at 98 °C and reaching to about 300 Hz at 21 °C is quite unusual.

These doubts can, however, be pacified after analyzing our sample (in the form of binary mixtures) under study. Important points related with the sample are as follows.

(1) The core group of 5* CBB is almost two times larger than that of 7OCB because 5* CBB has four phenyl rings whereas 7OCB has only two rings.

(2) CN is the main dipole bearing group in both the molecules (i.e., 5* CBB and 7OCB) and is attached at the terminals. However, in 5* CBB another dipole bearing group is COO but it is in the core. Hence net dipole moments of these two molecules are expected almost along their long axes [40].

(3) The mole ratio of 5* CBB and 7OCB in the sample is 0.2 and 0.8.

With these points in mind, we believe that two different modes of relaxation (M_1 and M_2) are due to the presence of two widely different types of molecules in our sample, as observed in a few other cases as well [42–45]. M_1 is due to 5* CBB whereas M_2 is due to 7OCB. The relaxation frequencies of mode M_1 are lower than that of M_2. This is because a molecule of 5* CBB is bulkier than the molecule of 7OCB and hence 5* CBB molecules experience larger hindrance than the molecules of 7OCB while rotating about their short axes. Unusually the low value of relaxation frequencies of mode M_1 at low temperatures especially in the N_{re}^* phase seem to be the combined effects of large sizes of the core group and/or even possible dimerization of 5* CBB molecules [46] coupled with high rotational viscosity at low temperatures. Such low values of relaxation frequencies have been reported for some other binary systems showing reentrant nematic phases [47]. A larger magnitude of dielectric strengths of mode M_2 as compared to that of mode M_1 (see Fig. 6) can be assigned to the larger mole percentage of 7OCB in the sample. One can guess that longitudinal component of dipole moment ($\mu_\parallel$) of a 5* CBB molecule may be slightly larger than that of 7OCB molecule due to the presence of additional COO group in 5* CBB. This may be one of the reasons that average ratio of $\delta\varepsilon_2$ and $\delta\varepsilon_1(\sim 3:1)$ is less than the mole ratio of 7OCB and 5* CBB (4:1). It is important to emphasize that mode M_2 could be separable from high-frequency effects of the cell as soon as its relaxation frequency came down in the MHz region in TGBA phase. Needless to say in the high-temperature cholesteric and isotropic phases M_2 could not be detected because of its further high relaxation frequencies (>2 MHz). The presence of mode M_1 could also be noticed on the dielectric spectrum as soon as it relaxation frequency came down to MHz region but due to its weak strength (as compared to that of M_2), it could not be possible to separate it out from high-frequency effects of the cell unless its relaxation frequencies came down to 200–300 kHz at about 98 °C.

Table I shows that sequence of activation energies of molecular rotation about their short axes (modes M_1 and M_2) is $(W_a)_{N^*} < (W_a)_{TGBA} < (W_a)_{N^*_{re}}$ This is a usual sequence because in the case of lower temperature mesophases, rotation of molecules becomes more and more difficult due to increase in the viscosity [47,48]. For the same reason, the activation energy of the reentrant cholesteric phase observed on the lower-temperature side of the TGBA phase is larger than the cholesteric phases observed on the higher temperature side. Nozoki *et al.* have also reported that activation energies of the reentrant nematic phase is higher than that of the nematic phase for a similar reason [41]. It is also important to note that activation energies observed here for chiral phases (N^*, TGBA, and N^*_{re}) are larger than their achiral counterparts (N, Sm-A, and N_{re}) reported by Nozoki *et al.* [41]. This effect can be assigned to two factors viz. the presence of chirality and the possibly high value of viscosity of the present sample.

B. Planar aligned sample

Subjecting the material to planar boundary conditions (discussed in Sec. III), results in an alignment of the molecules approximately parallel to the rubbing direction of the electrodes surfaces (planar alignment). In the case of chiral phases such as N^* and TGBA, their helical axes lie normal to the electrode surfaces under the condition of planar alignment. Optical texture of TGBA phase observed under this condition is most often similar to the one observed for the N^* phase, known as the Grandjean texture (uniform intensity) [19]. For the higher-temperature side of the TGBA phase of the present sample we have observed cholestericlike Grandjean texture but for completely stabilized TGBA phase we have recorded a texture shown in Fig. 7.

Measuring electric field applied through electrodes of a cell treated for planar alignment determines the component of dielectric permittivity parallel to the helical axis, i.e., normal to long axes ($\varepsilon'_\perp$) of the molecules. For isotropic liquid and N^* phases, corrected permittivity data are almost constant in the frequency range of 100 Hz to 1 MHz implying that there is no relaxation mode upto 10 MHz. However, in the TGBA phase we have noticed a weak mode of relaxation named $M_3(\delta\varepsilon_3 \sim 0.19)$ at 42 °C with its starting relaxation frequency at about 669 kHz. The relaxation frequency (f_{r3}) of this mode decreases with decrease in temperature as

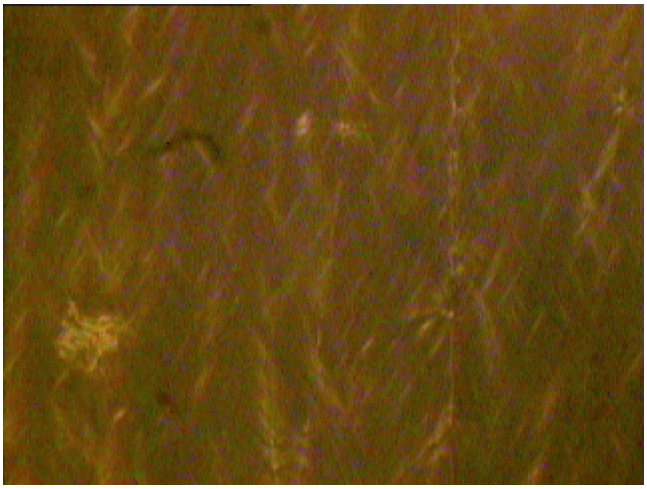

FIG. 7. (Color online) Optical texture of TGBA phase of planar aligned sample at 45.0 °C.

shown in Fig. 8. Dielectric strength ($\Delta\varepsilon_3$) initially increases up to 31 °C (max $\delta\varepsilon_3 \sim 0.42$) but thereafter decreases showing a diminishing trend of mode M_3 (see Fig. 9). The straight line drawn by the method of the least square fit of $\delta\varepsilon^{-1}$ versus T data for M_3 (Fig. 9) intercepts the temperature axis at 24.8 °C which agrees very well with the TGBA-N_{re}^* transition temperature analogous to the Sm-A^*-Sm-C^* transition of ferroelectric materials. In the light of previous experimental work [29–33] and, thereafter, the theory developed by Ismaili *et al.* [35], for the TGBA phase, M_3 has been identified as the soft mode relaxation of TGBA phase.

According to Eqs. (3) and (5), the slope of $\delta\varepsilon^{-1}$ with T is $\alpha/\varepsilon_0\chi_e^2C^2$ whereas that of f_r with T is $\alpha/2\pi\gamma_s$. The slope values of $\delta\varepsilon^{-1}$ and f_r with temperature for the soft mode of the TGBA phase of the present sample (5^*CCB+7OCB) are given in Table II along with the data obtained by Ismaili *et al.* for the homolog members of the $n\mathrm{F_2BTFO_1}M_7$ series. From Table II it is clear that the $d(\delta\varepsilon^{-1})/dT$ value for the present sample is almost the same as that for ninth and tenth

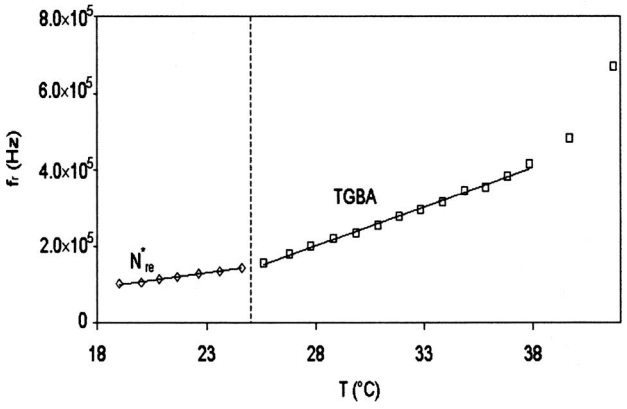

FIG. 8. Variation of relaxation frequencies f_r of mode M_3 with temperature T for planar aligned sample. The slope of the straight line obtained by least square fit of f_r with T gives df_r/dT mentioned in Table II. Broken vertical line represents TGBA-N^*_{re} transition temperature as reported in Sec. II.

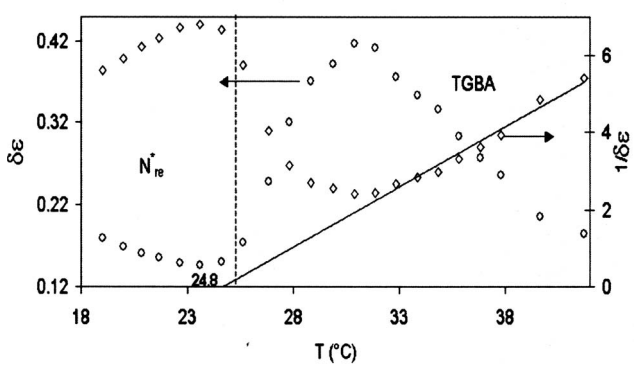

FIG. 9. Variation of dielectric strength ($\delta\varepsilon$) and inverse of the dielectric strength $(\delta\varepsilon)^{-1}$ of mode M_3 with temperature. Slope of the straight line obtained by least square fit of $(\delta\varepsilon)^{-1}$ with temperature T (shown by solid straight line) gives $(\delta\varepsilon)^{-1}/dT$ mentioned in Table II. Broken vertical line represents TGBA-N^*_{re} transition as mentioned in Sec. II. Broad nature of TGBA-N^*_{re} transition as mentioned there in Sec. II is clearly visible here also.

member of $n\mathrm{F_2BTFO_1}M_7$. However, the df_r/dT value is quite low compared to that of the $n\mathrm{F_2BTFO_1}M_7$ series. The difference in df_r/dT values for the present sample and that of $n\mathrm{F_2BTFO_1}M_7$ can be assigned to the difference of the soft mode viscosity γ_s of two different varieties of samples. It is reasonable to expect that γ_s for mixtures having different species of molecules may be higher than pure materials beside many other factors.

C. Effect of dc electric field

Application of the dc electric field plays important role in the study of collective and individual molecular dynamics. By applying an appropriate dc electric field it is possible to align the molecular (electrical) dipoles in the direction of the field. In the case of helical phases sufficient field strength can unwind even the helix. The effect of the dc field on a planar cell is depicted in Fig. 10 for the TGBA phase. During this experiment, the soft mode of the TGBA phase seems to be suppressed due to the application of a dc electric field similar to that observed by Xu *et al.* [31]. However, simultaneously a mode named M_4 appears (at a critical field of about $E_{C1} \sim 4 \pm 1$ kV/cm) for which relaxation frequencies are not too different from those of the soft mode (M_3) making it difficult

TABLE II. $\Delta\varepsilon^{-1}(T)$ and $f_r(T)$ versus temperature slopes for the soft mode of TGBA and Sm-A phases.

Phase/Material	$d(\Delta\varepsilon^{-1})/dT$ (°C^{-1})	df_r/dT (kHz °C^{-1})
TGBA (5^*CBB+7OCB)	0.27	30.4
TGBA ($9\mathrm{F_2BTFO_1M_7}$) [35]	0.23	50.5
Sm-A($9\mathrm{F_2BTFO_1M_7}$) [35]	0.07	14.3
TGBA ($10\mathrm{F_2BTFO_1M_7}$) [35]	0.29	54.3
TGBA ($11\mathrm{F_2BTFO_1M_7}$) [35]	0.48	41.3
TGBC ($11\mathrm{F_2BTFO_1M_7}$) [35]	0.43	49.8

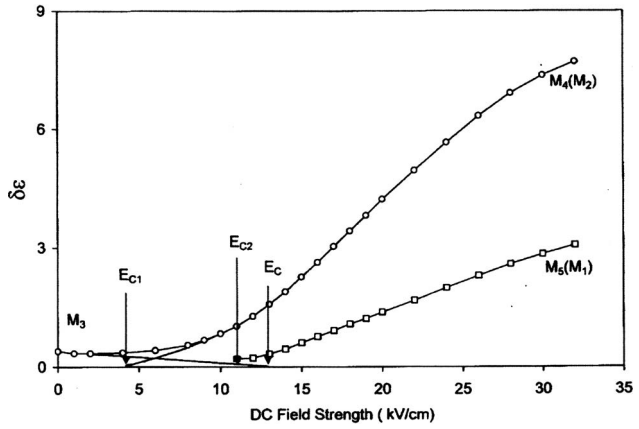

FIG. 10. Variation of dielectric strengths of modes M_3, M_4, and M_5 with dc field strength applied through the electrodes treated for planar alignment of the sample at 31.7 °C. E_{C1} and E_{C2} represent critical fields for the appearance of modes M_4 and M_5, respectively. Similarly E_C may be approximate as field strength required for the suppression of mode M_3.

to separate the two modes. Slightly above E_{C1}, another mode (named M_5) appears at another critical value of the field $E_{C2}=11\pm1$ kV/cm. For both these modes, the dielectric strength increases almost linearly with field strength (see Fig. 10).

In order to characterize these two modes, we carried out temperature-dependent dielectric measurements in N^*, TGBA, and N^*_{re} phases at a constant dc field strength of 30 kV/cm. Results of the experiment are shown in Figs. 1 and 11–15. Figure 14 shows that variations of the relaxation frequencies of two modes observed here (M_4 and M_5) are quite similar to those (M_2 and M_1) observed for homeotropic aligned sample (see Fig. 5). From Table I it is also clear that activation energies of M_4 and M_5 are almost equal to those of M_2 and M_1, respectively, in different phases. Hence we conclude that M_4 is M_2 and M_5 is M_1. But then the question arises of why these similarities exist? We believe that the presence of a dc field above a critical value tends to align molecules along its own direction by applying torque ($\tau=\mu E \sin\theta, \theta$ being angle between electric field $\vec{E}$ and net dipole moment $\vec{\mu}$ of the molecule). The existence of two

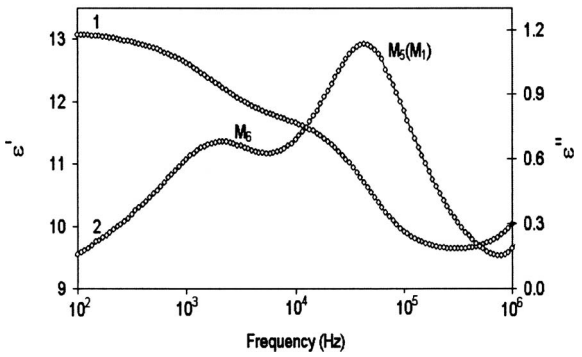

FIG. 11. Variation of relative permittivity ε' (curve 1) and loss ε'' (curve 2) with frequency for N^* phase (at 74.2 °C) with a dc electric field of strength 30 kV/cm applied across planar cell.

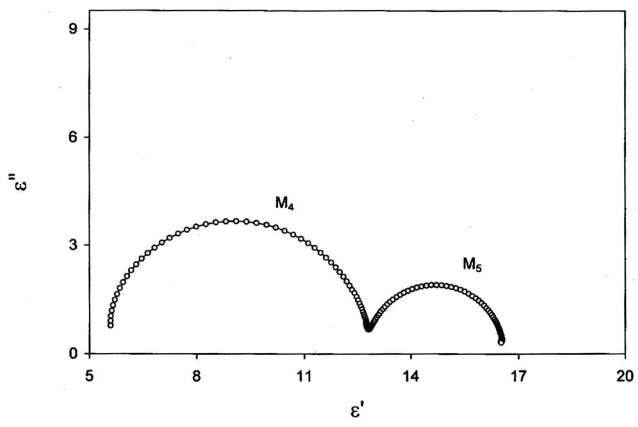

FIG. 12. Cole-Cole plot showing modes M_4 and M_5 of TGBA phase (31.7 °C) obtained with a dc electric field of strength 30 kV/cm applied across planar cell.

different values of critical field (E_{C1} and E_{C2}) are due to different lengths and dipole moments of 5* CBB and 7OCB molecules. With the increase in the field strength, molecules tend to align normal to electrode surfaces (i.e., homeotropically) from their original position (planar orientation). Here it is important that homeotropically aligned TGBA phase under the action of the dc field may be helix free (i.e., it will be equivalent to Sm-*A*) and we have verified this aspect by viewing a filament free almost perfectly dark field of view under the crossed polarizers. When the field is removed, the filamentary texture of Fig. 2 reappears but there is some time lag between removal of field and reappearance of filamentary texture. Although the relaxation frequencies of M_4 and M_5 agree with those of M_2 and M_1, respectively, the observed dielectric strengths, particularly those of M_4, are lower than the respective values of M_2 (see Figs. 6 and 15). This is because of the imperfect homeotropic alignment of molecules (at least near the bounding surfaces) due to insufficient field strength. This fact is visible in Fig. 10 where dielectric strengths of two modes are unsaturated even at a field strength of 32 kV/cm. We could not apply further high dc fields due to the instrumental limitations. Remarkably,

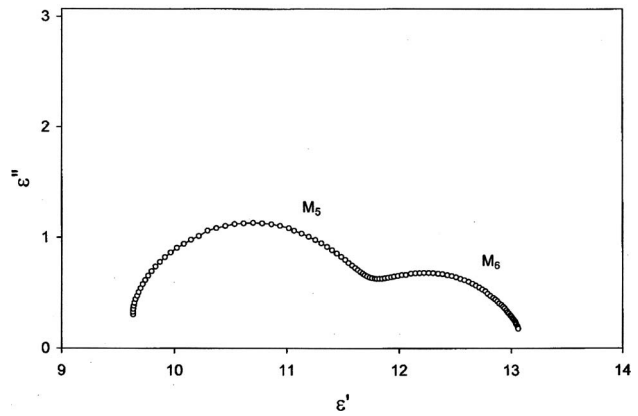

FIG. 13. Cole-Cole plot showing modes M_5 and M_6 of N^* phase (74.2 °C) obtained with a dc electric field of strength 30 kV/cm applied across planar cell.

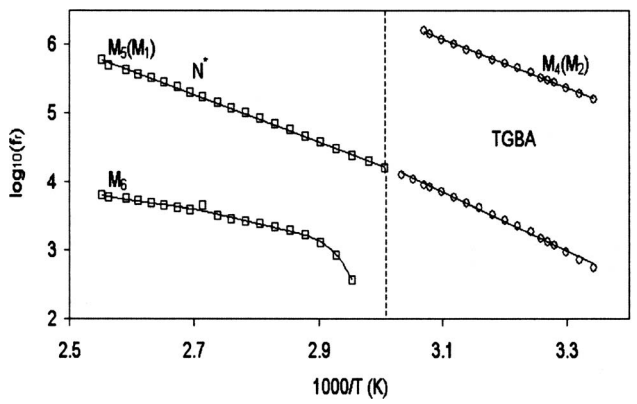

FIG. 14. Variation of relaxation frequencies of modes M_4, M_5, and M_6 with inverse of the temperature obtained with a dc electric field of strength 30 kV/cm applied across planar cell. Broken vertical line represents TGBA-N^* transition temperature as reported in Sec. II.

with the application of a dc field, it has been possible to detect mode $M_5(M_1)$ from 118 °C (see Figs. 14 and 15) which is much higher than the temperature at which M_1 is noticeable in the cell treated by lecithin (98 °C) as reported in Sec. IV A.

As discussed in Sec. IV A, M_4 (or M_2) is not detectable in the N^* phase here also because of its high relaxation frequencies. However, a mode named (M_6) is visible in the N^* phase in the kHz frequency region (see Figs. 11, 14, and 15). Here it is worthwhile to mention that M_6 appears only above critical field strength E_{C3}(=18 kV/cm) and its dielectric strength slowly increases with increase in field strength above E_{C3}. Although the dielectric strength of M_6 is low ($\delta\varepsilon \sim 1.6$ at a field strength of 30 kV/cm) but the range of relaxation frequencies and its variation with temperature (see Fig. 14) suggests the origin of this mode is due to some collective and not individual fluctuations of molecules. Logically it seems ridiculous to talk about some collective mode of relaxation in

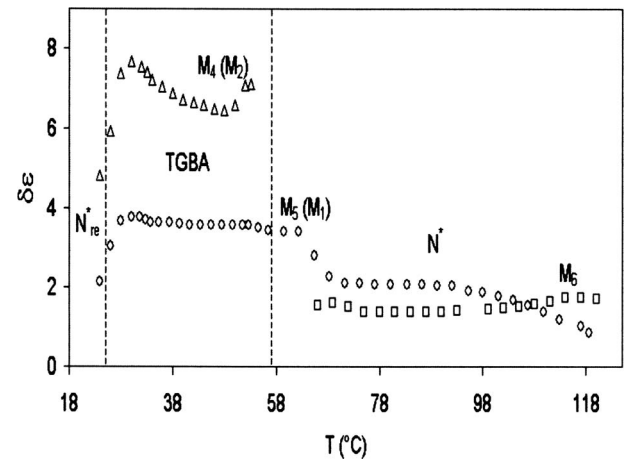

FIG. 15. Variation of dielectric strengths of modes M_4, M_5, and M_6 with temperature obtained with a dc electric field of strength 30 kV/cm applied across planar cell. The broken vertical lines represent TGBA-N^* and N^*_{re}-TGBA transition temperatures as reported in Sec. II.

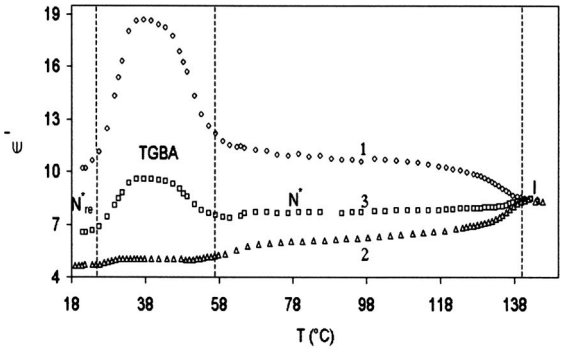

FIG. 16. Variation of $\varepsilon'_{\parallel}$ (curve 1), $\varepsilon'_{\perp}$ (curve 2) taken at 100 Hz, and $\varepsilon_{av}=(\varepsilon'_{\parallel}+2\varepsilon'_{\perp})/3$ (curve 3) with temperature. Broken vertical lines represent different transition temperatures reported in Sec. II. The broad nature of different transitions as mentioned in Sec. II is clearly visible here also.

the N^* phase for which dielectric strength increases with increase in field strength. However, it can be assigned to the deformation of the helix of the N^* phase under dc field [31].

We have also applied a dc field on a homeotropic cell and have observed that dielectric strengths of modes M_1 and M_2 slightly increase and the filamentary texture of the TGBA phase (Fig. 2) is converted into a perfect dark field of view at about 15 kV/cm. When the dc field is removed filamentary texture (i.e., helix) is restored. These effects explain that for TGBA phase, the helix unwinding field strength is 15 kV/cm. In the N^* phase, mode M_6 appears at about a critical field strength of 18 kV/cm (as observed for the planar cell) and thereafter it dielectric strength increases up to 30 kV/cm.

Figure 16 shows variations of static values of relative dielectric permittivities for homeotropic and planar aligned molecules represented by $\varepsilon'_{\parallel}$ and $\varepsilon'_{\perp}$, respectively, with temperature. 100 Hz data of $\varepsilon'_{\parallel}$ and $\varepsilon'_{\perp}$ have been taken as static values, i.e., $\varepsilon'_{\parallel}(0)$ and $\varepsilon'_{\perp}(0)$. This approximation $[\varepsilon'_{\perp}(0) \sim \varepsilon'_{\perp}(100)]$ is true for a planar oriented sample where relaxation frequencies of mode M_3 are well above 100 kHz at all temperatures of the measurement but not for a homeotropic aligned sample. In the case of homeotropic alignment, relaxation frequency of mode M_1 is as low as 300 Hz toward the lower-temperature side of the measurement and hence $\varepsilon'_{\parallel}(100) < \varepsilon'_{\parallel}(0)$ but we have no option as dielectric data below 100 Hz is not reliable, particularly for a homeotropic alignment. From Fig. 16 it is evident that mixture possess positive dielectric anisotropy, i.e., $\Delta\varepsilon' = \varepsilon'_{\parallel} \sim \varepsilon'_{\perp}$ is positive in all the mesophases. $\Delta\varepsilon'$ is the maximum in the TGBA phase at about 38 °C ($|\Delta\varepsilon'|_{max}=14$). However, $\Delta\varepsilon'$ decreases drastically at the TGBA-N^*_{re} transition and the anisotropy of the reentrant N^* phase becomes almost equal to that of the N^* phase ($\sim$5). It is important to mention here that $\Delta\varepsilon'$ for reentrant cholesteric and TGBA phases shown in Fig. 16 may be slightly lower than the actual values. This is because $\varepsilon'_{\parallel}(100) < \varepsilon'_{\parallel}(0)$ towards the lower-temperature side of the measurement as discussed earlier in this paragraph. The high value of the positive dielectric anisotropy in the present sample is the consequence of small angle between net dipole moments of the molecules and their long axes as discussed in

Sec. IV A. As visible in Fig. 16, $\varepsilon'_\perp$ decreases continuously with decrease in the temperature throughout N^*, TGBA, and N^*_{re} phases. According to Maier-Meier and other related theories of the static dielectric permittivity, generally $\varepsilon'_\parallel$ and $\varepsilon'_\perp$ both show increasing trend with decrease in temperature [49,50], however, in the present case $\varepsilon'_\perp$ is showing a mildly opposite behavior. There are some other cases where the completely unusual behavior of $\varepsilon'_\parallel$ and $\varepsilon'_\perp$ have been reported and explained on the basis of dipole-dipole correlations [51–53]. According to the minimum energy configuration, dipolar groups of molecules should be antiparallel to each other. With decrease in temperature, the separation of molecules decreases and hence antiparallel correlation of the transverse component of molecular dipoles may increase. This seems to be the cause behind the decrease of $\varepsilon'_\perp$ with decrease in temperature in the present binary system. Antiparallel correlation of longitudinal components of dipoles may not be much affected in this process as long as the sample is in the N^* phase and hence $\varepsilon'_\parallel$ shows usual variation with temperature. However, in the TGBA phase, the situation may change. Due to the packing requirement of molecules in smectic layers, now core groups of 5^* CBB molecules almost overlap (antiparallel dimer) and this has been confirmed by measuring the layer thickness in the case of binary mixtures in which one component is 7^* CBB [46]. In this process, the separation between end dipolar groups (CN) becomes very large and hence the antiparallel correlation of longitudinal components becomes almost zero. Thus $\varepsilon'_\parallel$ of the TGBA phase is increased as compared to the N^* phase. Value of $\varepsilon'_\parallel$ again comes down when the layered structure is destroyed and the system goes to a reentrant cholesteric phase from the TGBA phase. Another reason for the observed behavior of $\varepsilon'_\parallel(0)$ and $\varepsilon'_\perp(0)$ may be continuous improvement in the alignment of molecules with decrease in the temperature. There may be some other explanations for the observed behavior of $\varepsilon'_\parallel(0)$ and $\varepsilon'_\perp(0)$ in Fig. 16 and can be affirmative only after studying large number of such systems.

V. CONCLUSIONS

The binary mixture of 5^* CBB (0.2 mole) and 7OCB (0.8 mole) has a wide temperature range TGBA phase with a reentrant cholesteric phase. Dielectric spectroscopy of homeotropically aligned samples shows two modes of dielectric relaxations (M_1 and M_2) in TGBA and N^*_{re} phases corresponding to the individual rotation of 5^* CBB and 7OCB molecules about their short axis. In the N^* phase, M_2 could not be detected because of its weak strength and high relaxation frequencies. Soft mode relaxation due to the TGBA phase has been detected for planar oriented sample. Experimental values of the slopes of inverse of dielectric strength and relaxation frequencies with temperature $[d(\Delta\varepsilon^{-1})/dT$ and $df_r/dT]$ supports the recently proposed dielectric theory for the soft mode of the TGBA phase. By applying the dc electric field it has been possible to change planar orientation of molecules in the TGBA phase into a helix free homeotropic orientation. Mixture possess high values of positive dielectric anisotropy throughout N^*, TGBA, and N^*_{re} phases.

ACKNOWLEDGMENTS

We wish to thank Professor W. Kuczynski, Institute of Molecular Physics, Poznan (Poland) and Dr. S. K. Prasad, Centre for Liquid Crystal Research, Bangalore (India) for several fruitful discussions on experimental results. Thanks are also due to the University Grants Commission, New Delhi for financial assistance under a major research project.

[1] S. R. Renn, and T. C. Lubensky, Phys. Rev. A **38**, 2132 (1988).
[2] J. W. Goodby, M. A. Waugh, S. M. Stein, E. Chin, R. Pindak, and J. S. Patel, Nature (London) **337**, 449 (1989).
[3] O. D. Lavrentovich, Y. A. Nastishin, V. I. Kulishov, Y. S. Narkevich, and A. S. Tolochko, Europhys. Lett. **13**, 313 (1990).
[4] S. R. Renn and T. C. Lubensky, Mol. Cryst. Liq. Cryst. **209**, 349 (1991).
[5] S. R. Renn, Phys. Rev. A **45**, 953 (1992).
[6] M. Brunet, M. L. Navailles, and N. A. Clark, Eur. Phys. J. E **7**, 5 (2002).
[7] H. T. Nguyen, A. Bouchta, L. Navailles, P. Barois, N. Isaert, R. J. Twieg, A. Maaroufi, and C. Destrade, J. Phys. II **2**, 1889 (1992).
[8] I. Dierking, G. Giesselmann, and P. Zugenmaier, Liq. Cryst. **17**, 17 (1994).
[9] T. Chan, C. W. Garland, and H. T. Nguyen, Phys. Rev. E **52**, 5000 (1995).
[10] L. Navailles, C. W. Garland, and H. T. Nguyen, J. Phys. II **6**, 1243 (1996).
[11] L. Navailles, H. T. Nguyen, P. Barois, N. Isaert, and P. Delord, Liq. Cryst. **20**, 653 (1996).
[12] N. Isaert, L. Navailles, P. Barois, and H. T. Nguyen, J. Phys. II **4**, 1501 (1994).
[13] D. S. Shankar Rao, S. K. Prasad, V. N. Raja, C. V. Yelamaggad, and S. A. Nagamani, Phys. Rev. Lett. **87**, 085504 (2001).
[14] K. J. Ihn, A. N. Zasadzinski, R. Pindak, A. J. Slaney, and J. W. Goodby, Science **258**, 275 (1992).
[15] G. Srajer, R. Pindak, M. A. Waugh, J. W. Goodby, and J. S. Patel, Phys. Rev. Lett. **64**, 1545 (1990).
[16] L. Navailles, P. Barois, and H. T. Nguyen, Phys. Rev. Lett. **71**, 545 (1993).
[17] L. Navailles, R. Pindak, P. Barois, and H. T. Nguyen, Phys. Rev. Lett. **74**, 5224 (1995).
[18] L. Navailles, B. Pansu, L. Gorre-Talini, and H. T. Nguyen, Phys. Rev. Lett. **81**, 4168 (1998).
[19] W. Kuczynski, *Self-Organization in Chiral Liquid Crystals* (Scientific Publishers, OWN, Poznan, 1997).
[20] J. W. Goodby, in *Liquid Crystals II*, edited by D. M. P. Mingos (Springer-Verlag, Berlin, 1999), Vol. 95, pp. 83–147.
[21] H. S. Kitzerow, in *Chirality in Liquid Crystals*, edited by H. S. Kitzerow and C. Bahr (Springer-Verlag, Berlin, 2001), pp. 296–354.

[22] R. Dhar, Phase Trans. (to be published).
[23] W. Kuczynski and H. Stegemeyer, Mol. Cryst. Liq. Cryst. Sci. Technol., Sect. A **260**, 377 (1995).
[24] W. Kuczynski and H. Stegemeyer, Proc. SPIE **3318**, 90 (1997).
[25] M. Brodzik and R. Dabrowski, Liq. Cryst. **20**, 99 (1996).
[26] R. Dhar, M. B. Pandey, and V. K. Agrawal, Phase Transitions **76**, 763 (2003).
[27] R. Dhar, A. K. Srivastava, and V. K. Agrawal, Phase Transitions **76**, 959 (2003).
[28] R. Dhar, M. B. Pandey, and V. K. Agrawal, Mol. Cryst. Liq. Cryst. **409**, 269 (2004).
[29] H. T. Nguyen, C. Destrade, J. P. Parneix, P. Pochat, N. Isaert, and C. Girold, Ferroelectrics **147**, 181 (1993).
[30] C. Girold, C. Legrand, N. Isaert, P. Pochat, J. P. Parneix, H. T. Nguyen, and C. Destrade, Ferroelectrics **147**, 171 (1993).
[31] H. Xu, Y. P. Panarin, J. K. Vij, A. J. Seed, M. Hird, and J. W. Goodby, J. Phys.: Condens. Matter **7**, 7443 (1995).
[32] S. Wrobel, S. Hiller, M. Pfeiffer, M. Marzec, and W. Haase, Liq. Cryst. **18**, 21 (1995).
[33] F. Bougrioua, N. Isaert, C. Legrand, A. Bouchta, P. Barois, and H. T. Nguyen, Ferroelectrics **180**, 35 (1996).
[34] S. L. Srivastava and R. Dhar, Mol. Cryst. Liq. Cryst. Sci. Technol., Sect. A **317**, 23 (1998).
[35] M. Ismaili, F. Bougrioua, N. Isaert, C. Legrand, and H. T. Nguyen, Phys. Rev. E **65**, 011 701 (2001).
[36] M. B. Pandey, R. Dhar, V. K. Agrawal, R. Dabrowski, and M. Tykarska, Liq. Cryst. **31**, 973 (2004).
[37] S. L. Srivastava and R. Dhar, Indian J. Pure Appl. Phys. **29**, 745 (1991).
[38] S. L. Srivastava, Proc. Natl. Acad. Sci. (India) **63**, 311 (1993).
[39] R. Dhar, Indian J. Pure Appl. Phys. **42**, 56 (2004).
[40] N. E. Hill, W. E. Vaughan, A. H. Price, and M. Davies, *Dielectric Properties and Molecular Behavior* (Van Nostrand Reinhold London, 1969).
[41] R. Nozaki, T. K. Bose, and S. Yagihara, Phys. Rev. A **46**, 7733 (1992).
[42] F. Gouda, Ph.D. thesis, Dielectric Relaxation Spectroscopy of Chiral Smectic Liquid crystals (Department of Physics, Chalmers University of Technology, Goteborg, 1992).
[43] H. Kresse, H. Stettin, F. Gouda, and G. Anderson, Phys. Status Solidi A **111**, K265 (1989).
[44] M. I. Barnik, L. M. Blinov, A. V. Ivashchenko, and N. M. Shtykov, Sov. Phys. Crystallogr. **24**, 463 (1979).
[45] T. K. Bose, R. Chahine, M. Merabet, and J. Thoen, J. Phys. (France) **45**, 1329 (1984).
[46] M. Brodzik, R. Dabrowski, and J. Przedmojski, J. Phys. II **5**, 1805 (1995).
[47] S. Wrobel, M. Brodzik, R. Dabrowski, B. Gestblom, W. Haase, and S. Hiller, Mol. Cryst. Liq. Cryst. Sci. Technol., Sect. A **302**, 223 (1997).
[48] S. Urban, R. Dabrowski, B. Gestblom, and A. Kocot, Liq. Cryst. **27**, 1675 (2000).
[49] H. Kresse, *Advance Liquid Crystallography* (Academic, New York, 1983), Vol. 6, p. 109.
[50] L. M. Blinov, *Electro-Optical and Magneto-Optical Principles of Liquid Crystals* (John Wiley and Sons, New York, 1983).
[51] W. H. de Jeu, T. W. Lathouwers, and P. Bordewijk, Phys. Rev. Lett. **32**, 40 (1974).
[52] S. Chandrasekhar and B. R. Ratna, Mol. Cryst. Liq. Cryst. **82**, 193 (1982).
[53] S. L. Srivastava and R. Dhar, Mol. Cryst. Liq. Cryst. Sci. Technol., Sect. A **317**, 23 (1998).